Planktonic carbon cycling and transport in surface waters of the highly urbanized Hudson River estuary

Gordon T. Taylor,[1] *Juliette Way, and Mary I. Scranton*
Marine Sciences Research Center, Stony Brook University, New York 11794-5000

Abstract

   We examined variations in organic carbon (OC) pools and microplanktonic carbon fluxes at three stations in the Hudson River estuary during 12 cruises between Octobers of 1996 and 1998. Phytoplankton biomass and net primary production varied from 5 to 40 μmol C L^{-1} and 0.3 to 318.3 mmol C m^{-2} d^{-1}, respectively. Biomass and production of bacterioplankton in the surface layer commonly exceeded those of phytoplankton, varying from 0.2 to 72 μmol C L^{-1} and 1.4 to 70 mmol C m^{-2} d^{-1}, respectively. Median planktonic respiration varied from 275 to 605 mmol CO$_2$ m^{-2} d^{-1} between stations along the salinity gradient. Primary production/respiration (P:R) ratios varied temporally and spatially between 0.003 and 6.60, averaging 0.22. Carbon mass balances revealed that under low river discharges (<250 m^3 s^{-1}), the estuary processed 2.4-fold more carbon internally and advected 2.7-fold less carbon seaward than under higher flows. Annual OC budgets suggest that ~19 × 10^9 mol C yr^{-1} of total organic carbon (TOC) entered the estuary, whereas 30 × 10^9 mol TOC yr^{-1} was exported seaward, representing a net gain of 11 × 10^9 mol TOC yr^{-1} within the estuary. Microplankton processed ~32 × 10^9 mol C yr^{-1}, of which 5.6 × 10^9 mol C was attributed to photo- and chemoautotrophic (~72%) and heterotrophic (~28%) production; the remainder was respired to CO$_2$ (26.5 × 10^9 mol CO$_2$ yr^{-1}). The persistent imbalance between carbon oxidation and carbon fixation strongly suggests that the Hudson River estuary usually is net heterotrophic and is a significant source of inorganic carbon to the coastal ocean and atmosphere.

The notion that many aquatic systems are "net heterotrophic" has gained growing support from studies in a variety of environments. In this trophic state, oxidation of organic matter exceeds its production via autotrophy, because OC imported from more productive terrestrial systems subsidizes heterotrophic metabolism in receiving waters (Smith and Mackenzie 1987; Smith and Hollibaugh 1993). For example, measurements of plankton biomass, production, and respiration, and whole-lake gas fluxes strongly suggested that 20 oligotrophic Canadian lakes had a net heterotrophic carbon balance supported by allochthonous OC input from the local watershed (del Giorgio et al. 1999). In the tidal freshwater Hudson, as in other major rivers, investigations of plankton productivity, trophic structure, and CO$_2$ dynamics illustrate that rates of respiration of organic matter exceed its production at all times (Kempe 1982, 1984; Findlay et al. 1991; Howarth et al. 1992, 1996; Raymond et al. 1997). In nine European estuaries and the York River estuary, studies of CO$_2$ partial pressures (pCO$_2$) and dissolved inorganic carbon (DIC) have demonstrated that these systems are always supersaturated in CO$_2$ with respect to the atmosphere, a condition that can only be sustained if respiration surpasses primary production (i.e., P:R < 1) (Frankignoulle et al. 1996, 1998; Raymond et al. 2000).

   In order to understand the factors controlling trophic balance within estuarine systems, knowledge of organic carbon cycling is essential. Estuaries can function merely as conduits, discharging terrigenous materials largely untransformed to the coastal ocean, or they can function as biological and sedimentological filters, removing or transforming entrained materials. The fate and transport of OC pools depend on many factors, including the estuary's geomorphology, hydrologic residence time, turbulence, nutrient loading, temperature, ecology, and the OC's lability (Hopkinson et al. 1998; Howarth et al. 2000). Reports based on biochemical assessments suggest that TOC in estuaries should be very labile (50–60%) (Ittekkot 1988; Spitzy and Leenheer 1991). However, studies based on bioassays suggest that dissolved OC (DOC) lability actually is much lower (25–14% of total DOC) in riverine and marine samples (Søndergaard and Middelboe 1995). In the York River estuary, bioassays suggested that <8% of natural DOC is turned over within 1 month, the lower hydrologic residence time of this system (Raymond and Bauer 2000). Furthermore, DOC and particulate OC (POC) can behave nonconservatively during mixing between fresh and salt water, as well as independently of one another (Sañudo-Wilhelmy and Taylor 1999). In most studies, potentially important inputs (runoff, small tributaries, anthropogenic point sources, etc.) are poorly constrained or not even measured. For these reasons, differences in inventories of materials entering and leaving an estuary are poor indicators of total mass flux through the system. In addition to quantifying inventories, inflows, and outflows, some understanding of biological processing within the system is required to understand mass flux, and it is this which motivates the present study.

   Despite high TOC loadings, the balance between autotro-

phic and heterotrophic processes in estuaries varies spatially and temporally, controlled by wind-forced mixing, degree of stratification, light attenuation, freshwater discharge, tidal variations, and inorganic nutrient supply (Cole et al. 1992; Koseff et al. 1993; Howarth et al. 2000). In much of the Hudson River estuary (HRE), for example, the photic zone is shallow because of high turbidity. Suspended solids average 35 mg L^{-1} and can exceed 200 mg L^{-1}, and Secchi depths of <0.3 m are common (Arnold 1982; Sañudo-Wilhelmy and Taylor 1999). In addition, tidal and wind-driven mixing can be strong, deepening the mixed layer well below the photic zone and severely curtailing daily exposures of phytoplankton to photosynthetically active radiation (PAR). In fact, for at least the last 22 yr, inorganic N and P concentrations in the HRE have exceeded phytoplankton demand while light limitation and temperature have remained the major controls over primary production. This results in major nutrient plumes extending into the Mid-Atlantic Bight (Malone 1977; Hydroqual 1991).

The present study examines variability in organic matter pools (DOC, POC, and phytoplankton and bacterioplankton biomasses) and the major processes controlling them (autotrophic production, bacterial production, planktonic respiration, and river discharge) during a 2-yr field study of the HRE. Results are used to evaluate variability in the balance between autotrophic and heterotrophic processes, to better understand controls on carbon cycling within and carbon export from this important estuary and to construct a rudimentary carbon budget.

Materials and methods

Site description—The HRE, with contributions from the Hackensack, Passaic, and Raritan Rivers and Long Island Sound (Fig. 1), represents the largest freshwater source to the Mid-Atlantic Bight north of the Chesapeake Bay. Annual mean freshwater discharges of the Hudson alone between 1950 and the present have ranged from 17 to 52 × 10^6 m^3 d^{-1} (Howarth et al. 2000). Estimates of freshwater residence times vary from as low as 0.1–4 d (Howarth et al. 2000) to 15–60 d (Clark et al. 1992), depending on the area of the estuary included and freshwater discharge. In addition to relatively high loadings from nonpoint sources, the heavily urbanized HRE receives substantial discharges of municipal and industrial wastewater, because 88% of the >17 × 10^6 people (1980 census) residing in the watershed occupy the lower 13% of the entire watershed's area (metropolitan New York/New Jersey) (Suszkowski 1990).

Haverstraw Bay (HB) is the widest segment of the oligohaline estuary (65 km north of southern tip of Manhattan = river kilometer [rkm] 65) and has shallow flanks bordering the main channel that support modest amounts of submerged aquatic vegetation (Fig. 1). Station HB was located on the eastern edge of the main channel. Station GT (Grant's Tomb) was located just seaward of the largest water pollution control plant (WPCP) outfall in Manhattan (North River Plant) and seaward of the tidally driven turbidity maximum, a semipermanent feature of this estuary. This station was located within the salt wedge, on the eastern side of the chan-
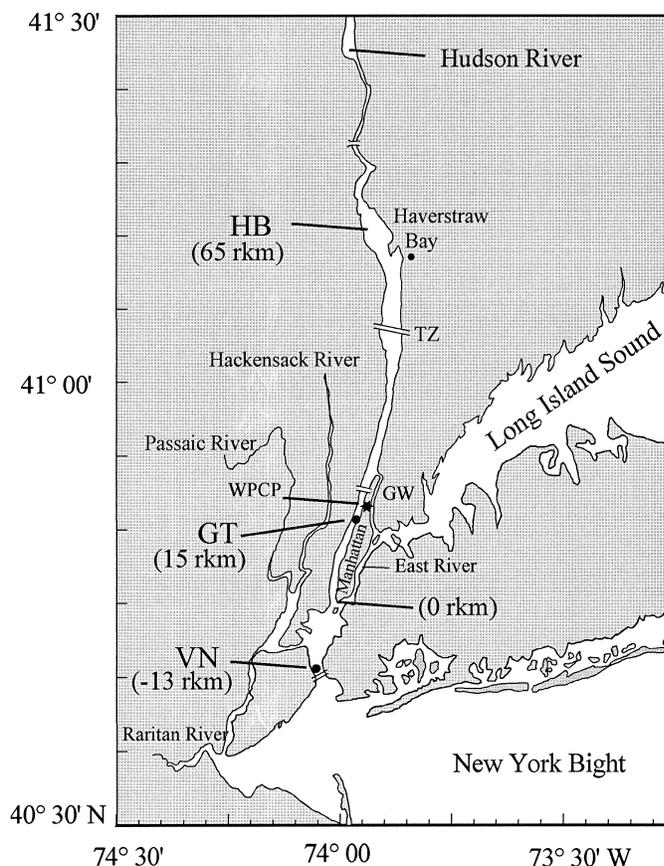
Fig. 1. Map of study site in the lower Hudson River estuary and New York/New Jersey Harbor complex. Sampling stations are Haverstraw Bay (HB; 41.22°N, 73.95°W), Grant's Tomb (GT; 40.81°N, 73.97°W), and Verrazano Narrows (VN; 40.61°N, 74.06°W). River kilometers (rkm) are relative to the Battery at the southern tip of Manhattan. GW and TZ, George Washington and Tappan Zee bridges; WPCP, North River sewage treatment plant.

nel (rkm 15; mean depth = 18.3 m). Station VN (Verrazano Narrows) was located just north of the bridge on the shipping channel's western margin (rkm −13) in ~19.5 m of water and represents our most marine station.

Sampling—Three-day cruises were staged aboard the R/V *Onrust,* operated by Stony Brook University. Hydrographic depth profiles for salinity, temperature, and dissolved oxygen were obtained with an AMS CTD package and YSI oxygen electrode attached to a General Oceanics sampling rosette. Discrete water samples were acquired in four 5-liter Niskin bottles from separate casts in surface, intermediate, and bottom waters. Before dispensing, all sample water from a single depth was pooled in a 22-liter Cubitainer® (Hedwin) and mixed well to minimize gravitational fractionation of particles. Pooling of samples from multiple Niskin bottles was necessary to accommodate the large array of analyses performed, of which only a subset is presented here.

Environmental parameters—Freshwater discharge, *q,* was calculated from the sum of daily rates reported from USGS-gauged stations in the Hudson River at Waterford, New

York, and in the Mohawk River at Cohoes, New York, both north of Troy Dam near Albany, New York (rkm 240) (http://waterdata.usgs.gov/ny/nwis/discharge). The lower Hudson is poorly gauged, but flow over Troy Dam is estimated to represent ~65% of the river's total freshwater budget (Howarth et al. 1991). Freshwater flow to HB and GT was estimated as $q_{corr} = q/0.65$. Freshwater discharge through Verrazano Narrows is dominated by the Hudson mainstem (87%), but also includes contributions from Long Island Sound via the East River and from Kill van Kull north of Staten Island (13%) (Hydroqual 1991; Brosnan and O'Shea 1996). Therefore, q_{corr} at station VN was estimated as $q/(0.65 \times 0.87)$. Total surface water discharge, Q, also includes saline bottom water entrained from tidal mixing. Q was calculated using the basin equation approach, assuming water and salt conservation, $Q = q_{corr}(S_{bot}/[S_{bot} - S_{surf}])$, where S_{bot} and S_{surf} are salinities in bottom and surface waters.

POC/DOC/nutrients—Samples for POC and DOC were collected in a separate 0.5-liter Niskin bottle whose entire volume was processed as a single sample. This approach compensated for sampling bias introduced by time-dependent settling of particles occurring in larger Niskin bottles. The entire Niskin sample was transferred to a clean glass bottle and passed through a precombusted GF/F filter shipboard. After rinsing the receiving flask with filtered sample, an aliquot of the filtered sample was acidified and stored at 5°C in a precombusted 40-ml EPA sample bottle with an acid-washed Teflon-lined cap until analysis for DOC. DOC was measured using a Shimadzu TOC-5000 Total Organic Carbon Analyzer (Sharp et al. 1995). Filters were stored frozen until analysis. POC and particulate organic nitrogen (PON) were analyzed on a fraction of the filter by combustion in a Carlo Erba EA1108 CHNS-O analyzer (Martin 1993).

Water samples for nutrient analyses were filtered through Whatman GF/F glass fiber filters and stored frozen in polyethylene bottles for dissolved inorganic nutrient analysis. Ammonium, nitrate, nitrite, and phosphate were analyzed by Chesapeake Biological Laboratory's Nutrient Analytical Services (University of Maryland) using automated colorimetric techniques described by Parsons et al. (1984). All nutrient and carbon concentrations were corrected with appropriate blanks (filters or reagents).

Phytoplankton biomass—Chlorophyll *a* (Chl *a*) and pheopigment concentrations were determined fluorometrically on 90% acetone extracts of particles from triplicate 0.1-liter subsamples retained on Whatman GF/F filters (Parsons et al. 1984). Phytoplankton biomass was estimated assuming a C : Chl *a* constant of 58, as previously determined for local estuarine communities by Tantichodok (1990), who derived biomass estimates using cell volume measurements of major taxa, and the Strathmann (1967) equations.

Bacterial biomass—Bacterioplankton abundances were measured using epifluorescence microscopy employing 4′,6-diamidino-2-phenylindole (DAPI) staining of samples preserved with 2% borate-buffered formaldehyde and captured

on 0.2-μm black polycarbonate membranes (Osmonics) (Porter and Feig 1980). To determine biovolumes of bacteria, 200 randomly selected cells in each sample were visually sorted into eight size classes based on their linear dimensions, approximated with an ocular micrometer at $\times1{,}000$ magnification. Cellular carbon biomass (C) was estimated from biovolume (V) using an allometric carbon to volume extrapolation function ($C = 0.12V^{0.72}$; Norland 1993). Cell carbon content estimates varied from 23.4 to 47.8 fg C cell^{-1} (mean $\pm$ 1 SD = 35.1 $\pm$ 7.2) between samples and were in excellent agreement with Fukuda et al.'s (1998) direct chemical determinations of 22.1–47.9 fg C cell^{-1} (30.2 $\pm$ 12.3) for coastal bacterial communities elsewhere.

Primary production—Samples for primary production were collected from the middle of the surface mixed layer, usually at dawn, and placed in quadruplicate 250-ml polycarbonate bottles, each inoculated with 5 μCi of Na$_2$H^{14}CO$_3$, and individual bottles were subjected to one of four light levels (neutral density screen pouches providing 56.7, 37.5, and 2.5% of surface irradiance [I_0] and a dark bottle). Samples were incubated for the remainder of the photoperiod in a deckboard flow-through water bath. Samples were processed in accordance with Parsons et al. (1984) using 0.22-μm cellulosic filters (Osmonics), including analysis of extracellular organic ^{14}C (EO^{14}C). EO^{14}C was determined by acidifying the 0.22-μm filtrate (0.1 N H$_3$PO$_4$ final conc.) in the field and then sparging samples with N$_2$ in the laboratory for 2 h. Duplicate aliquots of the residual nonvolatile, acid-stable organic ^{14}C were then radioassayed. EO^{14}C contributed from 0 to 86% of the total ^{14}C assimilation reported and averaged 26 $\pm$ 27%. Total assimilation rates were corrected with time zero blanks and dark bottle values for both PO^{14}C and EO^{14}C pools. To estimate specific activity of the tracer, total DIC was computed from observed salinity by assuming conservative mixing within the salinity gradient. DIC concentrations in the tidal freshwater Hudson are usually ~1.0 mmol C (Raymond et al. 1997). For the marine end member, DIC concentrations were calculated from salinities according to Parsons et al. (1984). The assumption of DIC conservation is reasonable because pH is typically >7.4 throughout the entire estuary (R. Ranheim, New York Dept. Envir. Protection, pers. comm. 2000; Raymond et al. 1997).

Most experiments were carried out over an entire photoperiod, but when unfeasible, diurnal net primary production (NPP) was scaled from hourly ^{14}C assimilation rates to the photoperiod. Attenuation of PAR (k_t) was estimated from Secchi depth measurements (Z_s in meters) at each station using $k_t = 1.5/Z_s$, a relationship empirically determined for turbid waters by Pilgrim (1987). Unless light saturation was suggested from ^{14}C assimilation data (e.g., rates observed at 56.7% I_0 equaled those of 37.5% I_0), production was assumed to be a linear function of I_0 and equal to 0 at 0.1% I_0. In cases of possible light saturation, photosynthesis was assumed constant from the depth of 37.5% I_0 to the surface. ^{14}C assimilation rates were depth-integrated to the 0.1% I_0 level using observed assimilation rates at the three light levels, by extrapolating photosynthetic response to 100, 1.0, and 0.1% I_0 and deriving simulated incubation depths from imposed light levels. Simulated incubation depths (Z_i) were cal-

culated as $Z_i = -[\ln(I_i/I_0)]/k_t$, where I_i/I_0 is the proportion of surface PAR at depth Z_i. Diurnal NPP was calculated by trapezoidal integration from observed and extrapolated ^{14}C rates positioned at their simulated depths. Extending the simulated photic zone to 0.1% I_0 increased integrated production rates by no more than 6% over rates integrated to 1% I_0.

Heterotrophic bacterial production—Bacterial net production (BNP) was estimated using both ^3H-Thymidine (Tdr) incorporation into DNA (Bell 1993) and ^3H-Leucine (^3H-Leu) incorporation into protein (Kirchman 1993). Separate 100-ml samples were inoculated with 0.1 ml of either 20 μmol L^{-1} ^3H-Tdr (methyl ^3H-Tdr; 52 Ci mmol^{-1}; 20 nmol L^{-1} final conc.; Amersham TRK 637) or 100 μmol L^{-1} ^3H-Leu (4,5-^3H-leu; 40–60 Ci mmol^{-1}; 100 nmol L^{-1} final conc.; Sigma L 800) and were incubated for 3 h at ambient temperatures in a darkened flow-through water bath. ^3H-Tdr and ^3H-Leu incubations were terminated by preserving in either 2% formaldehyde (final conc.) or 5% trichloroacetic acid (TCA; final conc.), respectively. Samples were stored at 5°C until processed. Replicate samples from one depth at each station were fixed with 2% formaldehyde for ^3H-Tdr or 5% TCA for ^3H-Leu prior to radioisotope addition to serve as T_0 adsorption blanks. T_0 blanks were stored and processed in parallel with all other samples. After each cruise, ^3H-Tdr samples were processed for ^3H-DNA production according to Bell (1993). Cell production was estimated using 1×10^{18} cells mol^{-1} Tdr on the basis of calibration studies with freshwater Hudson River communities reported by Findlay et al. (1991). Carbon production was estimated from the ^3H-Tdr incorporation data by multiplying the cell production by estimates of average cell biomass determined microscopically (described above). ^3H-Leu samples were processed for production of ^3H-protein according to Kirchman (1993) and extrapolated to carbon production using 3.1 kg C mol^{-1} leucine.

BNP based on ^3H-Tdr incorporation was significantly correlated with ^3H-Leu–based estimates but was systematically higher (Tdr = 0.40 + 1.52Leu; $r = 0.74$; $p < 0.001$; $n = 107$). The coherence of these independent estimates suggests that both techniques measured bacterial community growth, but the variance between them suggests that either the relationship between radioisotope incorporation and cellular production varied widely or the techniques measure growth processes that are weakly coordinated at the community level. Both postulates are probably true. The systematically higher ^3H-Tdr–based BNP suggests that the commonly used extrapolation factors are either too high for the ^3H-Tdr estimates or too low for the ^3H-Leu estimates. Alternatively, isotopic dilution of leucine, not measured here, might have been nontrivial and depressed apparent rates of ^3H-Leu incorporation (Simon and Azam 1989). Another possibility is that all bacterial populations within these communities might not experience balanced growth simultaneously, whereby specific rates of nucleic acid and protein synthesis are equivalent. Consequently, estimates of BNP used in comparison with NPP and in our carbon budgets are the mean of ^3H-Tdr and ^3H-Leu values, assuming that true bacterial production lies between these values.

Microplanktonic respiration—Microbial respiration was determined by continuous measurements of oxygen decrease in samples held in a newly developed automated respirometer. To remove most resuspended sediment and larger particles and organisms (evaluated below), 10–15-liter samples were first passed through tandem wound fabric filter cartridges (5 and 1 μm nominal pore sizes) by gravity flow and shaken gently to aerate. These filtered samples were dispensed into 2-liter sterile hospital intravenous (IV) bags (non-DEHP vinyl, Secure™ Medical), taking care to eliminate all visible bubbles, and then placed in a flow-through water bath. This approach, first described by Coffin et al. (1993), obviates the need for many biochemical oxygen demand (BOD) incubation bottles and eliminates atmospheric exposure during sampling because subsamples are periodically withdrawn from collapsible vessels. In our system, water is withdrawn at programmed intervals from each bag through its own solenoid valve, passed through a shared manifold to a flow-through O_2 microelectrode (Lazar Laboratories) immersed in the water bath, and finally pumped through a peristaltic pump and discharged. The respirometer automatically acquired time courses of O_2 consumption from 16 samples in series and recorded electrode potential from an aerated reservoir of distilled water (calibrant) and the water bath. Incubation temperatures were also recorded automatically using a submerged thermocouple. Data were postprocessed to correct for probe response drift (ΔmV μmol^{-1} O_2 h^{-1} in calibrant), variations in salinity between samples, and variations in water bath temperature. Although our setup minimized temperature variations and gas diffusion across vessel walls, O_2 concentrations were corrected for inward diffusion on the basis of empirical determinations of diffusive fluxes as a function of concentration gradients across IV bag surfaces and temperature (Taylor unpubl. data). Chemical oxygen demand (COD) was monitored in formaldehyde-killed samples.

Respiration rate is estimated as the maximum slope of oxygen depletion regressed against time and corrected for inward diffusion and COD. Statistically significant ($p < 0.05$) regressions included 5–12 time points and yielded correlation coefficients (r^2) between 0.47 and 0.99 (mean = 0.90). Uncertainty for respiration rates is presented as standard error (SE) of the regression slope. Corrections for O_2 diffusion into samples added as much as 40% to the rates. The precision and sensitivity of this experimental approach were sufficient to detect subtle differences in microbial activity. In validation experiments using two samples with contrasting respiration rates, mean relative standard deviation within treatments incubated in triplicate was 12% ($n = 82$).

To estimate respired CO_2 from O_2 consumption, a respiratory quotient (RQ = $\Delta CO_2 : -\Delta O_2$) was applied. Theoretical RQs based on elemental stoichiometry of plant material and metabolites vary from 0.67 to 0.97, but the consensus is that the RQ for heterotrophic breakdown of phytodetritus lies between 0.71 and 0.77 (Redfield et al. 1963; Anderson 1995; Robinson and Williams 1999). Community-level metabolic studies suggest that planktonic RQs lie between 0.71 and 0.88, depending on the system's productivity (Robinson et al. 1999; Søndergaard et al. 2000). Oceanographic models of elemental regeneration rates based on nutrient profiles and
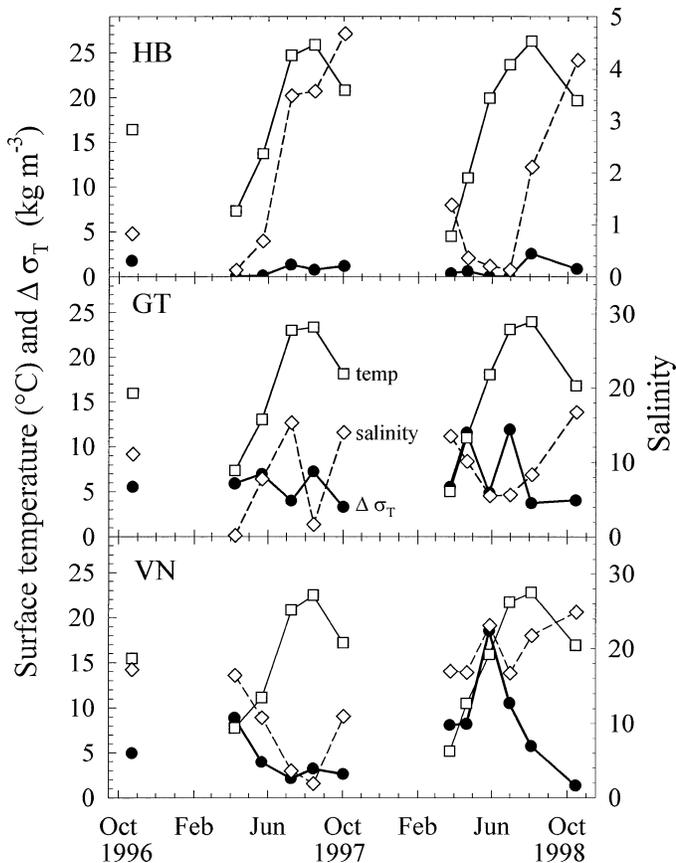
Fig. 2. Temporal variations in temperature and salinity in surface mixed layer and water stratification (expressed as density difference between surface and bottom waters, $\Delta\sigma_T$) measured at stations HB, GT, and VN.

elemental fluxes in aphotic waters suggest that realized RQs are lower, 0.61–0.62 (Takahashi et al. 1985; Martin et al. 1987). The lower RQs are indicative of O_2-consuming processes that do not result in CO_2 production, such as nitrification (Søndergaard and Middelboe 1995; Robinson and Williams 1999). On the assumptions that estuarine OC is of relatively low quality and that nitrification occurs in our samples, we employed a conservative RQ of 0.70.

Results

Environmental conditions—In HB channel (mean depth = 8.1 m), surface salinities and temperatures varied seasonally from 0.13 and 4.68‰ and from 4.5 to 26.3°C, respectively (Fig. 2). Little stratification was evident in this area. Density differences between surface and bottom waters ($\Delta\sigma_T$) were small, varying from 0.01 to 2.50 kg m^{-3} and were typically ~0.78 (Fig. 2). Chemical and biological properties were uniform from surface to bottom on almost all occasions, signifying a turbulent system. Although seasonal temperature trends were very similar for the two years, this station appeared to be less saline in 1998 than in 1997, consistent with slightly higher river discharge during the 1998 observation period.

At station GT, surface salinities and temperatures varied seasonally from 0.21 and 17.22‰ and from 5.0 to 27.0°C, respectively (Fig. 2). A high degree of stratification was evident in this area; $\Delta\sigma_T$ varied from 3.74 to 11.88 kg m^{-3} (mean = 6.20), and the halocline was evident at depths of 1.8 to 7.0 m (mean = 3.1 m), depending on river discharge and tide. Seasonal temperature trends were similar to HB, whereas salinity appeared more variable, probably because sampling was not confined to a particular tidal phase.

Surface salinities and temperatures at station VN also varied seasonally from 1.94 and 24.92‰ and 5.2 to 22.8°C, respectively (Fig. 2). VN was usually highly stratified, with $\Delta\sigma_T$ varying from 1.34 to 18.55 kg m^{-3} (mean = 6.56), with the halocline first evident at depths of 3.0–12.5 m (mean = 5.5 m).

Freshwater discharge, q, was most variable in winter and spring, with an annual range of 110 to 4,044 m^3 s^{-1} at the Troy Dam (Fig. 3A). Freshwater discharge observed from 1 Oct 96 to 30 Sept 97 was ~12% higher than during the comparable period for 1997–1998. However, median daily discharge in the 1997 sampling season (168 m^3 s^{-1}) was significantly lower than in the 1998 season (218 m^3 s^{-1}) (Fig. 3A, dashed lines). Six of our cruises occurred when q was <220 m^3 s^{-1} and six when q was above this value, but none coincided with peak discharge (Fig. 3A).

The photic zone tended to deepen from spring to fall in both years at all three stations (Fig. 3B). This deepening coincided with lower river discharge but was not systematically accompanied by increases in stratification, probably as a consequence of sustained tidal and wind mixing (Fig. 2). Variations in particle loading and water color might account for changes in water clarity. Estimates of the 1% I_0 light levels at HB and GT were similar for most observations, varying from 1 to 4 m, and were consistently shallower than at VN, which varied between 2.5 and 8.5 m. In more than 90% of our observations, the photic zone (Z_p) was shallower than the surface mixed layer (Z_m) (Fig. 3B,C). The $Z_p : Z_m$ ratio varied from 0.13 to 0.45 (mean = 0.26) at HB, from 0.13 to 1.33 (mean = 0.69) at GT, and from 0.33 to 3.38 (mean = 0.89) at VN. Therefore, phytoplankton exposure to light was probably suboptimal for most of the photoperiod at all stations because of continuous mixing out of the photic zone.

Carbon pools—DOC concentrations in the surface mixed layer tended to decrease along the salinity gradient ($r^2 = -0.13$, $p < 0.01$) between HB and VN, but most of the variance was not explained by salinity (Fig. 4A). The considerable scatter around the regression line suggests that processes beyond mixing of coastal water (low DOC) with river water (high DOC), such as external loadings and in situ processes, influence DOC distributions. Concentrations varied from 136 to 777 μmol C L^{-1} with no apparent seasonality. In 1997, median DOC concentrations (216 μmol C L^{-1}) in surface waters were significantly lower (t-test, $p < 0.05$) than in 1998 (282 μmol C L^{-1}) among all stations. At HB, DOC concentrations were indistinguishable between sampling depths, indicating a well-mixed water column. In the majority of observations at GT and VN, DOC in surface waters equaled or exceeded those in intermediate or bottom
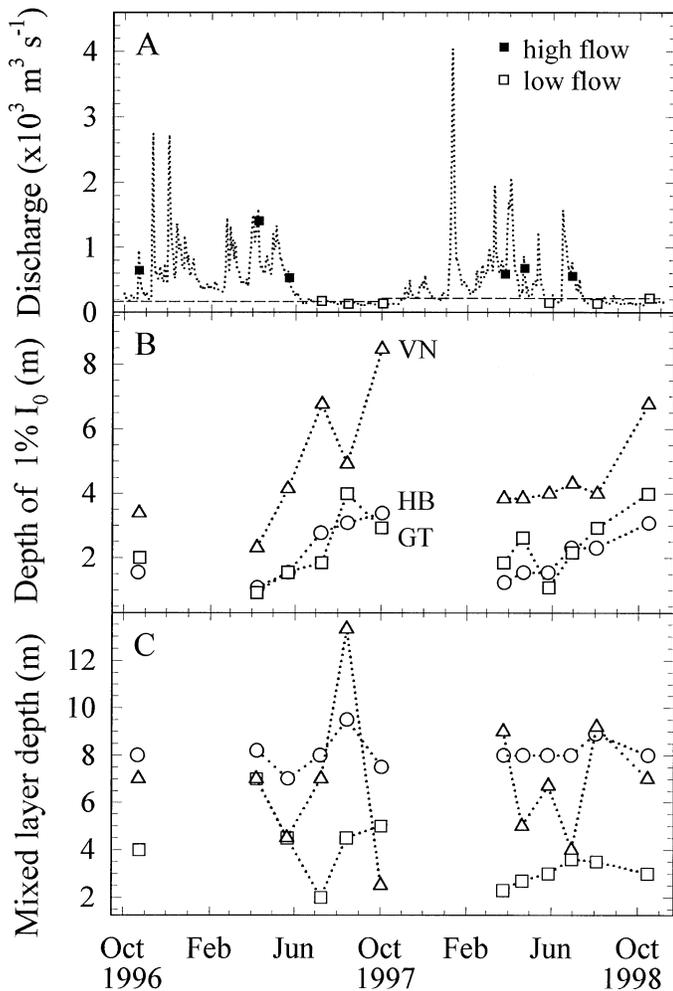
Fig. 3. Temporal variations in (A) river discharge summed from USGS gauged station 01335754 in the Hudson River at Waterford, New York, and station 01357500 in the Mohawk River at Cohoes, New York, both located north of Troy Dam near Albany, New York; (B) depth of photic zone, considered to be depth of 1% I_0; and (C) mixed layer depth determined from CTD and dissolved O_2 profiles. Horizontal lines in panel A are spring through fall daily medians. Squares in panel A denote sampling dates.

Fig. 4. Variations in (A) dissolved and (B) particulate organic carbon pools along the salinity gradient in the surface mixed layer between stations HB, GT, and VN. All depths are included for HB because CTD data demonstrate homogeneous mixing throughout the water column. Open symbols, 1996–1997 samples; closed symbols, 1998 samples; solid diamonds, halocline and bottom water values for GT and VN (presented for comparison). Error bars represent precision (± 1 SD) associated with analysis of triplicate subsamples.

waters, suggesting that DOC supply to surface waters was generally higher (Fig. 4A).

POC concentrations in surface waters appeared to decrease slightly with salinity (Fig. 4B). However, the relationship is weak ($p > 0.05$), suggesting that distributions were controlled more by OC processing within the estuary. Highest concentrations were observed at GT when salinities were between 5 and 9‰, perhaps because of flocculation of DOC. Among all observations, concentrations varied between 13 and 321 μmol C L^{-1} and were relatively invariant temporally. As with DOC, POC concentrations were essentially the same in surface, intermediate, and bottom waters at station HB. At GT, however, in 10 of 12 observations, POC concentrations were consistently highest in bottom waters and lowest in surface waters, suggesting that sediment resuspension or point discharges (outfalls) at depth were important sources of POC to this segment of the estuary.

Biomass—Typical of turbid, energetic estuaries, phytoplankton biomass was relatively low in surface waters at all stations, varying from 1.0 to 8.2 μg Chl *a* L^{-1} or 5 to 40 μmol C L^{-1} (Fig. 5). Standing stocks varied seasonally, presumably controlled by water clarity, stratification, mixing, grazing, and sedimentation because nutrients never appeared depleted; mean ($NH_4^+ + NO_3^- + NO_2^-$) = 38.7 μmol N L^{-1}, range = 1.2–70.3; mean PO_4^{3-} = 2.4 μmol P L^{-1}, range = 0.7–4.6. Consistent with its higher $Z_p : Z_m$ ratios (Fig. 3), station VN supported the largest phytoplankton biomasses during all but one observation. Station GT consistently had the lowest phytoplankton biomasses.

Spatial and temporal distributions of bacterial abundances were markedly different from those of phytoplankton (Fig. 5). Bacterial abundances were almost always highest at HB and were significantly lower, but similar at GT and VN, where bacterioplankton tended to increase from spring
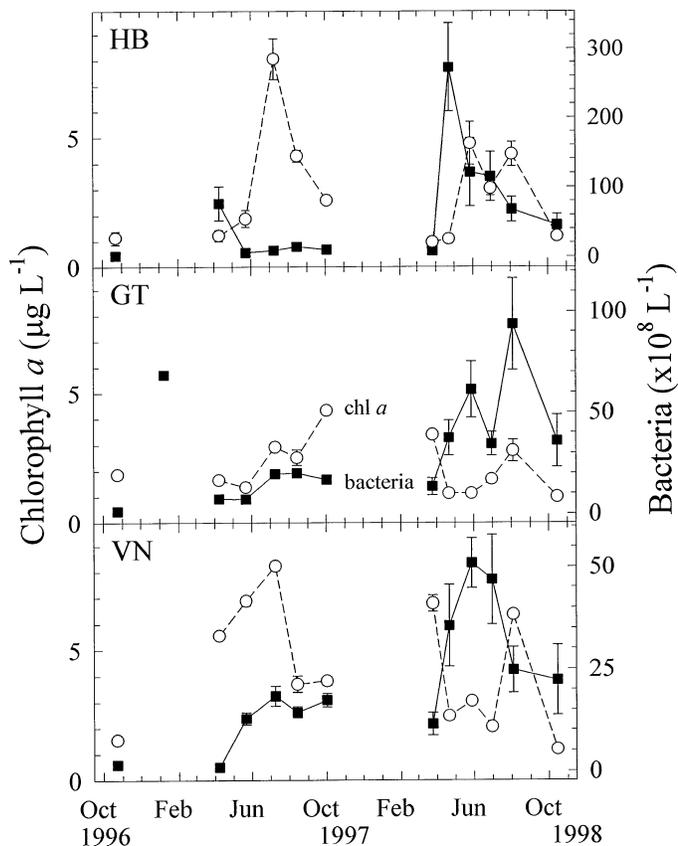
Fig. 5. Temporal variations in Chl *a* concentrations and bacterioplankton abundances in surface mixed layer at stations HB, GT, and VN. Error bars represent ±1 SD for triplicate filtrations (Chl *a*) and for enumeration within ≥10 microscopic fields of a single membrane (bacteria). Error bars for many samples do not exceed widths of symbols.

through summer. In further contrast to phytoplankton, median bacterial abundances in 1997 were significantly (*t*-test; $p < 0.001$) lower at all stations than in 1998; 16 versus 100, 12 versus 46, and 11 versus 32×10^8 cells L^{-1} at HB, GT, and VN, respectively. Accurate enumeration of higher trophic levels, specifically flagellated protozoa, was hampered by the copious debris in the viewing field of these larger samples and therefore is not presented.

Perhaps the most striking difference between years was the change in relative contributions of bacteria and phytoplankton to our biomass inventories. In 1997, bacteria contributed 12 to 22% to the total (bacteria + phytoplankton), whereas in 1998, they contributed between 40 and 68%. In both years, bacteria at VN contributed less to biomass inventories than at stations higher in the estuary, where proportions were similar to one another.

Photoautotrophic production—Diurnal NPP was relatively low throughout the system, varying from 0.3 to 318 mmol C m^{-2} d^{-1}, and increased seaward (Fig. 6). NPP was significantly correlated with Secchi depths ($r = 0.64$, $p < 0.001$), the $Z_p:Z_m$ ratio ($r = 0.48$, $p < 0.005$), PO_4 concentrations ($r = 0.41$, $p < 0.015$), and inversely with N : P ratios ($r = -0.44$, $p < 0.01$), but not with any inorganic nitrogen spe-
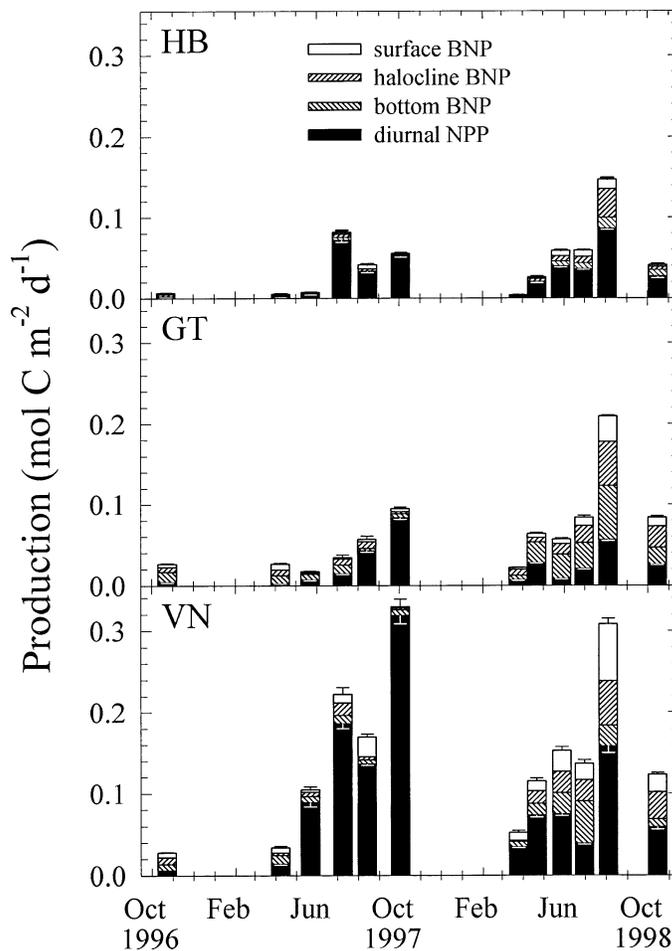
Fig. 6. Temporal variations in diurnal net primary production integrated over the photic zone and bacterial net production (mean from ^{3}H-Leu and ^{3}H-Tdr determinations) integrated through surface, halocline, and bottom layers at stations HB, GT, and VN. Error bars represent ±1 SD and account for error propagated through integrations of all light levels or layers, each subject to its own error: relative error $= (\sigma_a^2 + \sigma_b^2 + \sigma_c^2)^{0.5}/(a + b + c)$.

cies. NPP was highest in late summer and not significantly different between years, averaging 31 at HB, 25 at GT, and 99 mmol C m^{-2} d^{-1} at VN for all observations.

Heterotrophic production—Bacterioplankton net production (BNP) exhibited strong seasonality, increasing from spring into summer and then decreasing by October (Fig. 6). Like NPP, BNP generally increased seaward. BNP was not significantly correlated with DOC or POC concentrations, and less than half the variance was explained by temperature ($r = 0.48$, $p < 0.001$), suggesting that lability or rate of supply of substrates might exert more control than TOC pool size or temperature. Unlike NPP, but similar to DOC concentrations and bacterial biomass, BNP in 1997 was significantly lower ($p < 0.05$) at all stations than in 1998. Median BNP integrated over the entire water column averaged 5 and 17 at HB, 17 and 53 at GT, and 21 and 71 mmol C m^{-2} d^{-1} at VN in 1997 and 1998, respectively. Thus, bacterioplankton accounted for a smaller proportion of the total micro-
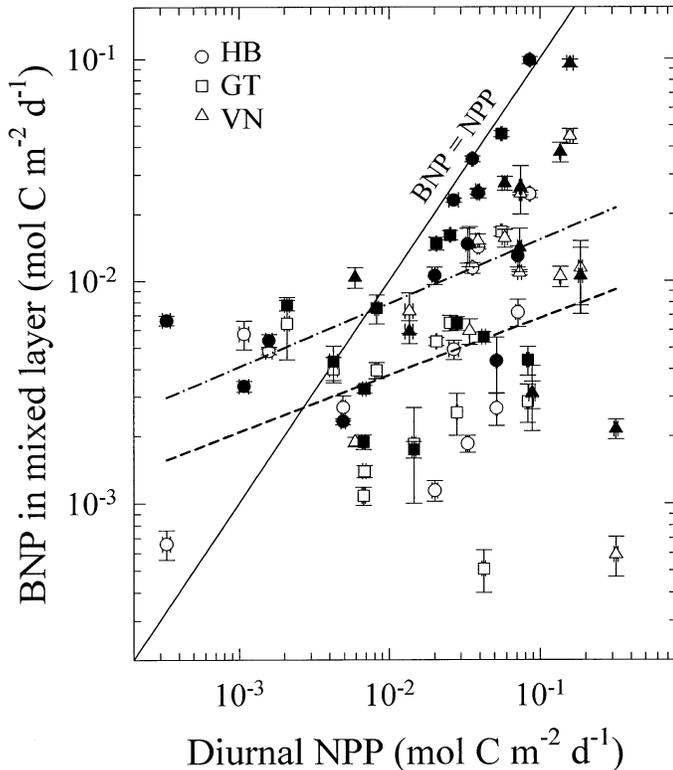
Fig. 7. Comparison of areal rates of bacterial net production and diurnal net primary production in the surface mixed layer at all stations. Solid symbols, BNP measured by ^{3}H-Tdr; open symbols, BNP measured by ^{3}H-Leu. Broken lines are least squares regressions for both data sets, neither of which is significant ($p > 0.05$). Vertical error bars represent ± 1 SD of triplicate BNP measurements, and horizontal error bars represent ± 1 SD for integrals derived from three light levels measured in duplicate.

Fig. 8. Example of automated respirometer's data output from the cruise staged on 27–29 May 98 for stations HB, GT, and VN. Chemical oxygen demand was assessed from sample preserved with 2% formaldehyde at T_0 (HB). Gradient in oxygen concentrations between water bath and samples within IV bags calculated from difference between interior and exterior $[O_2]$ (GT). Dynamic response of system was assessed by OC amendment of a duplicate sample at T_0 with excess Difco yeast extract (VN). Regression lines for each depth or treatment were derived from diffusion-corrected data (not shown) to calculate O_2 consumption rates.

plankton production in 1997 than in 1998 (27 vs. 36; 59 vs. 72; and 18 vs. 50% at HB, GT, and VN, respectively).

BNP integrated over the entire water column exceeded diurnal NPP in 18 of the 36 observations (Fig. 6). In the stratified segment of the estuary, however, strong coupling between surface layer processes and BNP in underlying waters cannot be assumed. Therefore, we confine comparisons of heterotrophic and autotrophic production to the mixed layer. Only in the unstratified segment of the estuary (e.g., HB) is the entire water column considered the mixed layer.

Overall, NPP was a poor predictor of bacterial production in the mixed layer because NPP was not significantly ($p > 0.05$) correlated with BNP, whether measured by ^{3}H-Tdr or ^{3}H-Leu incorporation (Fig. 7). In plotting BNP against NPP, we found ~84% of the observations were below the 1:1 line, illustrating that POC production by phytoplankton usually exceeded that of bacterioplankton in this system (Fig. 7). These estimates, however, do not account for carbon consumed by bacterial or algal respiration.

Respiratory fluxes—An example of data acquired by the automated respirometer is presented in Fig. 8. At the initiation of experiments, O_2 concentrations were at or near saturation and sometimes remained there for as long as 15 h,

until undetected air bubbles were completely consumed. Then $[O_2]$ decreased linearly until either labile OC or O_2 became limiting to heterotrophic metabolism. Despite extreme care to eliminate bubbles when filling IV bags, results suggest that about half our experiments were initiated under O_2 supersaturation conditions. Chemical oxygen demand was not evident in this sample (i.e., slope for formalin control was essentially zero and was usually <10% of total O_2 demand in other samples; Fig. 8-HB panel).

Even though the water bath was O_2-saturated, its $[O_2]$ oscillated in response to changes in the salinity and temperature of water pumped through the incubator (Fig. 8-GT panel). Therefore, inward O_2 diffusion had to be estimated at each time point from temperature and the O_2 gradient between the water bath and individual samples to derive O_2 consumption rates (regression lines in Fig. 8). In the OC-
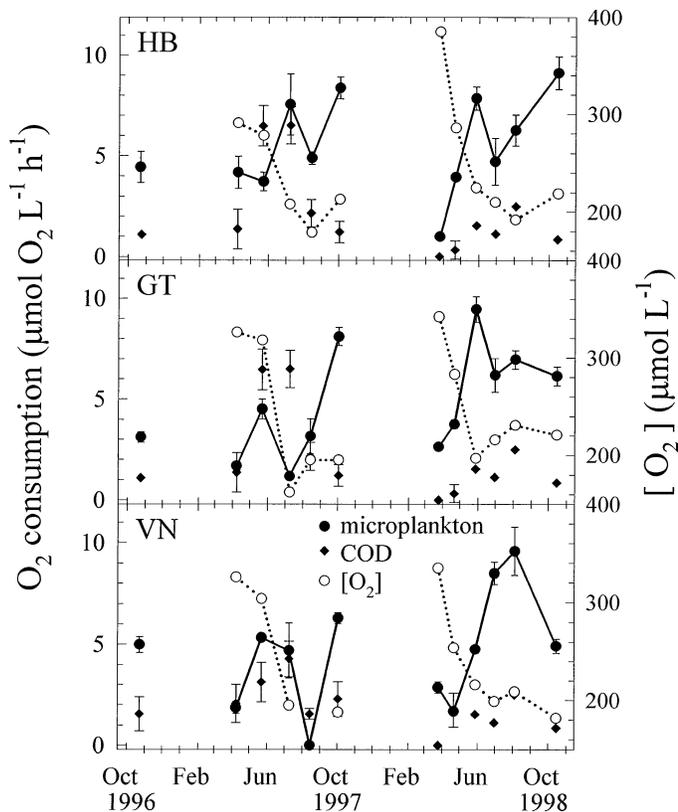
Fig. 9. Temporal variations in microplanktonic respiration, chemical oxygen demand, and dissolved O_2 measured in the surface mixed layer at stations HB, GT, and VN. Error bars represent the SE of regression slopes (see Fig. 8).

amended samples (positive control), $[O_2]$ remained below 50 μmol O_2 L^{-1} for ~112 h and then increased about sevenfold (arrow in Fig. 8-VN panel). At this point, the O_2 concentration gradient was steep, and rates of inward O_2 diffusion exceeded those of O_2 consumption, probably because labile material was exhausted by bacterial metabolism.

With few exceptions, respiration rates in the halocline and bottom waters were similar to one another, but usually lower than in surface waters, indicating lower metabolic rates at depth. Respiration rates in surface waters varied from undetectable to 9.6 μmol O_2 L^{-1} h^{-1}, and the relative standard error averaged 11% for all field respiration estimates ($n = 36$). Respiration tended to increase from spring through summer at all stations (Fig. 9), but only about half the variance is explained by water temperature ($r = 0.54$, $p < 0.001$). Dissolved O_2 concentrations in surface waters varied between 162 and 385 μmol O_2 L^{-1}, systematically decreasing from spring through fall at all stations (Fig. 9). Variations in dissolved O_2 reflect differences in the balance between solubility, physical ventilation, and oxygen demand (biological + chemical).

The original intent of the respiration assay was to measure bacterioplankton respiration exclusively. However, sieving whole water through 5- and 1-μm wound filter cartridges permitted ~40% of total Chl *a* to pass into respiration samples. Heterotrophic nanoflagellates were also observed microscopically in preserved filtrate. Therefore, measured ox-

ygen consumption includes contributions from most bacteria, small phytoplankters, and a portion of the protozoan community. It probably excludes particle-associated bacteria and the majority of the microzooplankton, which could add on the order of 10–20% to measured respiratory demands based on typical biomass relationships. Consequently, respiration rates should be considered minimum estimates of microplanktonic respiration. Respiration covaried with BNP to some extent, whether measured by ^{3}H-Tdr ($r = 0.46$, $p < 0.01$) or ^{3}H-Leu ($r = 0.44$, $p < 0.01$) and, to a lesser extent, with NPP ($r = 0.35$, $p < 0.05$), suggesting that bacteria dominate measured oxygen demand. The potential respiratory demand of phytoplankton is explored below.

Inorganic carbon fluxes—In productive aquatic systems, CO_2 consumption by primary producers must exceed CO_2 production by respiration to be considered net autotrophic. Clearly this is almost never the case within the HRE (Fig. 10). Our conservative areal rates of microplanktonic respiration in surface waters almost always exceeded those of CO_2 assimilation by a large margin. In most cases, photoautotrophic assimilation only consumed a small portion of the CO_2 produced. Without respiration measurements, the net heterotrophic carbon balance would not be apparent from consideration of bacterial and phytoplankton production alone.

An additional, nontrivial biological sink for CO_2 in this system appears to be dark DIC assimilation, DCA (Fig. 10). These fluxes were calculated from net production of $PO^{14}C$ and $EO^{14}C$ in the primary productivity dark bottles and were integrated over the mixed layer. Rates at HB and VN were similar, varying from 0 to 130 and 0 to 240 mmol C m^{-2} d^{-1}, respectively, but were routinely higher at GT (0–3,200 mmol C m^{-2} d^{-1}). Control experiments verified that production of $PO^{14}C$ and $EO^{14}C$ in these incubations was, in fact, biological. DCA can occur through anaplerotic carboxylation reactions performed by all organisms and through chemoautotrophy, presumably performed by nitrifying bacteria in this system. Potential contributions of these processes are discussed below.

Discussion

Net heterotrophy—Our observations clearly demonstrate that the saline reach of the HRE is a predominantly heterotrophic system, as has been previously shown for the tidal freshwater reach of this system (Findlay et al. 1991; Howarth et al. 1992, 1996; Raymond et al. 1997). Although carbon oxidation rates almost always exceeded rates of organic carbon production, the relative balance between autotrophic and heterotrophic processes varied spatially and temporally. The more stratified, less turbid, high-Z_p:Z_m station, VN, tended to have the highest photoautotrophic contribution, but inclusion of DCA revealed that GT was just as likely to have a net autotrophic balance (Fig. 10). In contrast, the carbon balance at HB, the station with highest DOC concentrations and poorest light environment, was always overwhelmingly net heterotrophic. Carbon imbalances tended to increase through the summer because respiration increased more rapidly than autotrophy. However, bacterial abundances, BNP, and DOC

concentrations did not exhibit consistent seasonal trends. These variables were weakly correlated with one another and with respiration. The higher values observed in 1998 might have been, in part, an artifact of our sampling schedule (i.e., timing of sampling relative to episodic rainfall and discharge events) rather than evidence of interannual variability (explored below).

Findlay et al. (1991) reported a summer seasonal average BNP of 192 mmol C m^{-2} d^{-1} for a portion of the tidal freshwater Hudson River that supports diurnal NPP of 20–40 mmol C m^{-2} d^{-1} (Cole et al. 1991). Even without explicitly considering respiration, this reach of the river (rkm 65–228) is clearly net heterotrophic. For the entire water column at our oligohaline station (HB), estimates of bacterial production derived from the ^{3}H-Leu technique varied from 0.7 to 24 mmol C m^{-2} d^{-1} (mean = 6.8). Considering that diurnal NPP varied from 0.3 to 86 mmol C m^{-2} d^{-1} (mean = 31) here, most bacterial production could be supported by autochthonous production if phytoplankton respiration and herbivory were ignored, if bacterial growth efficiencies were moderate ($\geq$25%), and if only ^{3}H-Leu estimates were considered. However, the higher estimates derived from the ^{3}H-Tdr technique for the same station (from 2.3 to 98 mmol C m^{-2} d^{-1}; mean = 20), suggest that these waters are net heterotrophic, regardless of phytoplankton carbon loss terms and bacterial growth efficiencies. We note that our BNP rates are significantly lower than ^{3}H-Tdr–based rates reported for the tidal freshwater reach of the Hudson River by Findlay et al. (1991), a finding consistent with higher DOC concentrations observed in the riverine portion of this system.

Our range for microplanktonic oxygen consumption (undetectable to 9.6 μmol O$_2$ L^{-1} h^{-1}; Fig. 9) was comparable to that reported using similar techniques for bacterioplankton alone at estuarine and coastal stations on the Gulf of Mexico (0.1–6.1 μmol O$_2$ L^{-1} h^{-1}; Coffin et al. 1993). From these rates and ambient O$_2$ concentrations, we estimate that dissolved O$_2$ pools in surface waters turned over as slowly as 0.1 d^{-1} in March and as rapidly as 1.4 d^{-1} in August. On average, dissolved O$_2$ at all stations turned over at 0.76 d^{-1}, indicating that O$_2$ replenishment generally exceeded planktonic respiration rates. Given the observed low NPP and high turbulence, physical ventilation must drive O$_2$ replenishment to a greater extent than photosynthetic O$_2$ production. It seems likely that the 14-fold seasonal range in O$_2$ turnover reflects the variance in metabolic rates more than seasonal changes in O$_2$ solubility, which only varied by a factor of 1.6.

Comparing microplanktonic respiration with NPP and BNP clearly demonstrates that heterotrophic processes dominate carbon fluxes in the estuarine Hudson River (Fig. 10). In only 5 of 36 observations did CO$_2$ consumption exceed CO$_2$ production. At all other times, respiration exceeded autotrophic production by factors of 1.1 to 340, underscoring the importance of allochthonous organic matter in fueling heterotrophs in this estuary. At HB, respiration rates applied to the entire water column varied from 112 to 936 mmol C m^{-2} d^{-1} and averaged 592 $\pm$ 260 mmol C m^{-2} d^{-1} ($\pm$1 SD; Fig. 10). This is consistent with previous estimates by Howarth et al. (1992), who used a whole-ecosystem approach and found that planktonic respiration varied over a similar
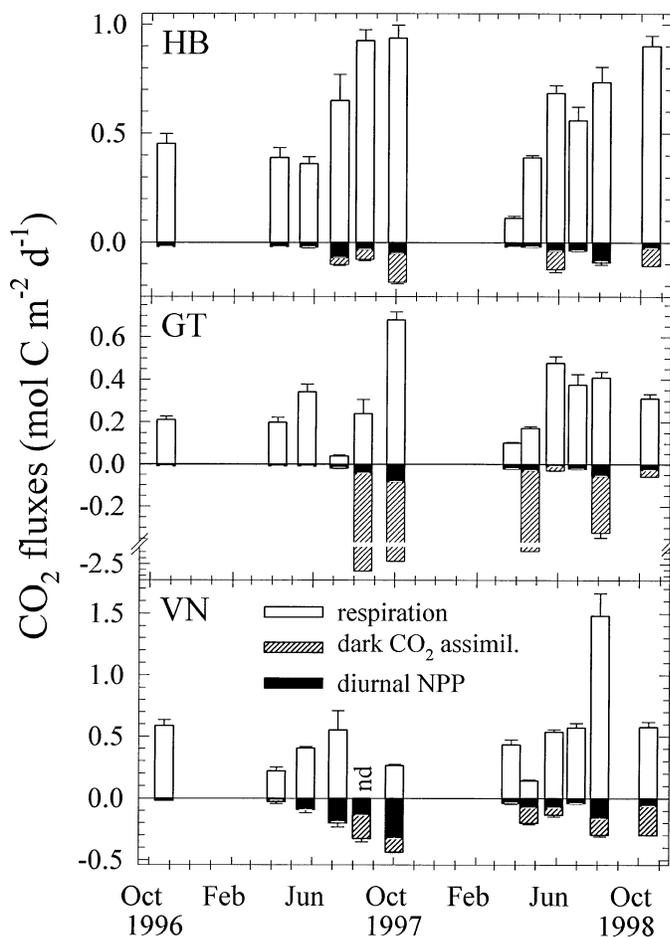
Fig. 10. Temporal variations in biologically mediated CO$_2$ fluxes in the surface mixed layers of stations HB, GT, and VN. Positive values represent CO$_2$ production and negative represent consumption. CO$_2$ production rates were estimated from O$_2$ respiration rates integrated over the surface mixed layer and assuming an RQ of $0.7 \Delta CO_2 : -1 \Delta O_2$ (see text). CO$_2$ consumption is the sum of NPP integrated over the photic zone and dark carbon assimilation integrated over the surface mixed layer. Error bars represent $\pm$1 SD and account for error propagated through integrations (see Fig. 6). nd, not determined.

range from 117 to 750 mmol C m^{-2} d^{-1} in a 40-km stretch of the tidal freshwater Hudson River (rkm 122–162). Using a refinement of this approach further downriver in the mesohaline reach (rkm 19–35), Swaney et al. (1999) demonstrated that system respiration could be as high as 1,100 mmol C m^{-2} d^{-1}. We believe that our respiration rates are conservative, because O$_2$ supersaturation, evident at initiation of some respiration incubations, might have masked more rapid O$_2$ depletions when the most labile OC was consumed. Coffin et al. (1993) observed that [O$_2$] in samples from Gulf of Mexico estuaries was most rapidly depleted in the first 10 h of containment. Furthermore, we have employed a conservative RQ (0.7 ΔCO_2 : -1 ΔO_2), and some microplankton respiration was excluded by sieving (discussed below). Factoring in these three limitations, microplanktonic respiration rates could be $\geq$30% higher than reported.

In a cross-system analysis of lakes, rivers, and oceans, Søndergaard and Middelboe (1995) reported predictable relationships between total and labile DOC, which was estimated from the amount of carbon supporting bacterial growth and respiration. In the Hudson, however, BNP and respiration rates, alone or summed together, were not significantly correlated ($p > 0.05$) with the DOC/POC concentrations or particulate $C:N$ ratios. To evaluate whether absence of correlations could have resulted from temperature effects on respiration and DOC consumption, we applied a Q_{10} of 2.5 to normalize all metabolic data to a constant temperature of 25°C, but this only marginally improved correlations with DOC and POC pools ($p > 0.05$). Supply of labile substrates apparently prevailed over temperature as the primary determinant for microheterotrophic metabolism. As recently demonstrated by Raymond and Bauer (2000) in the York River estuary, labile bacterial substrates appear to be small, but dynamic, fractions of DOC and POC pools in estuaries. They reported that variability in labile DOC was undetectable by total DOC measurements, probably owing to the complexity of multiple sources and sinks in estuaries. Consequently, simultaneous measurement of bacterial production and respiration remains a better proxy for organic matter lability in estuaries than extrapolation from total DOC concentrations.

Factors contributing to net heterotrophy—In turbid, well-mixed rivers and estuaries where mixing depth often exceeds critical depth, $Z_m > Z_{cr}$, phytoplankton's residence time in the photic zone is considerably less than the photoperiod because of downwelling (Lucas et al. 1998). According to the Sverdrup critical depth model, when $Z_m > Z_{cr}$ persists, NPP is curtailed because phytoplankton's rate of carbon fixation is outpaced by its daily integrated respiration. Obviously, experimental conditions for measuring NPP in estuaries seldom mimic conditions experienced by phytoplankton in nature. Of necessity, subsamples are maintained under constant light conditions for most of the photoperiod, allowing time for photoadaptation that is not afforded to in situ cells transported through the mixed layer (e.g., Alpine and Cloern 1992; this study). Therefore, rates that conceptually integrate diurnal NPP over a static photic zone might overestimate the true rates for highly dynamic systems. Furthermore, diel (24 h) NPP must be considerably lower than diurnal rates because phytoplankton respiration is continuous. Cole et al. (1991) deduced that phytoplankton respiration could not amount to much more than 5% of light-saturated hourly primary production per unit Chl *a* (P^b_{max}) if NPP were to be, in fact, positive within the tidal freshwater Hudson River. Similarly, Jensen et al. (1990) concluded from regression analysis that hourly phytoplankton respiration amounted to ~6% of gross primary production in a shallow, eutrophic Danish estuary. Although the true magnitude and variability of phytoplankton respiration and the influence of photoadaptation are unknown, we conclude that our estimates of diurnal NPP are probably higher than in situ rates.

These concerns aside, estimates of diurnal NPP at HB and GT (Fig. 6) averaged 31 and 25 mmol C m^{-2} d^{-1}, respectively, and are in very good agreement with those reported by Cole et al. (1991) for stations between Haverstraw Bay

and Castleton, New York (rkm 228). NPP in the more saline and stratified portion of the estuary (VN) was considerably higher, averaging 99 mmol C m^{-2} d^{-1}, presumably resulting from lower turbidity and higher $Z_p:Z_m$ ratios here than up-river. Factoring in phytoplankton respiration yields negative diel NPP values for 16 of 36 observations. On average, inclusion of respiratory losses reduced diurnal NPP rates by 62, 155, and 87% at HB, GT, and VN, respectively, over a diel cycle. Such comparisons suggest that either the 5% P^b_{max} assumption is too high or that net diel production is negative on occasion. In fact, diel NPP was negative in 9 of 12 cases at GT, which also represents a poor light environment for phytoplankton (rapid mixing and high turbidity). Although these respiratory losses are substantial portions of the phytoplankton carbon budget, they represent a trivial fraction of total planktonic community respiration (0.09–11%), averaging 3% of total measured respiration. The relatively low diurnal rates of NPP and the downward adjustment of these numbers resulting from respiratory losses underscore the subordinate role of photoautotrophs in the carbon cycle of the Hudson estuary.

Dark DIC assimilation—An unexpected finding from our ^{14}C primary productivity studies was the unusually high DIC assimilation frequently observed in the dark bottles at GT. We postulate that nitrification was more important than anaplerotic carboxylation in samples with significant DCA. To illustrate, anaplerotic carboxylation in the TCA cycle could only account for 0.1 to 22% of DCA (mean = 9%) for all samples with DCA rates $\geq$5 mmol C m^{-2} d^{-1} ($n = 19$), if we assume that as much as 8% of the total measured biological production (NPP and BNP) is thus derived (Li 1982). In low-DCA samples (<5 mmol C m^{-2} d^{-1}), however, anaplerotic carboxylation could account for most observed DCA (41–100%; mean = 95%). Furthermore, rates were highest at GT and VN, which consistently had high NH_4^+ concentrations (7–24 and 15–33 μmol L^{-1}, respectively). In fact, DCA was positively correlated with NH_4^+ ($r = 0.38$, $p < 0.03$), the first electron donor in nitrification and even more strongly with NO_2^- ($r = 0.58$, $p \ll 0.001$), an intermediate electron donor.

GT and VN are seaward of a large outfall (~6.4 × 10⁵ m³ d⁻¹ discharge) from New York City's North River WPCP. In the Potomac estuary, WPCP plumes have been implicated as sites of nitrification on the basis of elevated production of N_2O (McElroy et al. 1978). In the highly polluted Scheldt estuary, abundances of cultivable nitrifying bacteria covaried with gradients in NH_4^+, NO_2^-, and NO_3^- downstream of WPCP outfalls (Billen 1975). Trends in alkalinity and nutrients along the Scheldt's salinity gradient were also consistent with substantial nitrification occurring in this estuary (Frankignoulle et al. 1996). These trends result from either the presence of nitrifiers in the discharge, or from in situ growth of nitrifying bacteria stimulated by input of reduced nitrogen species.

Nitrifying bacteria are an integral part of secondary wastewater treatment, oxidizing NH_4^+ produced through ammonification within the plant. However, the high NH_4^+ loadings in the HRE might signify the inefficiency of this process locally. Anthropogenic inputs of reduced nitrogen species

Table 1. Summary of Spearman rank order correlations between Hudson River freshwater discharge, q, at Troy Dam and physical, chemical, and biological variables in the mixed layer at stations HB, GT, and VN. Sample size = 36 for all comparisons.

Variable versus q	Correlation coefficient, r	Significance, P
Light attenuation coefficient, k	0.449	<0.006
NO_2^-*	−0.512	<0.002
PO_4^{-3}*	−0.526	<0.002
Phytoplankton biomass	−0.412	<0.020
Diurnal NPP	−0.646	≪0.001
Planktonic respiration, R	−0.633	≪0.001
Dark C assimilation	−0.634	≪0.001
NO_3^-,* NH_4^+,* DOC, POC, Bacterial biomass, BNP	n.s.†	>0.050

Note: All significant correlations (P<0.02) appear not to have arisen by chance (i.e., by type I errors). Likelihood of type I errors was tested with sequential Bonferroni test (Rice 1989).

* Inorganic nutrients measured by standard automated colorimetry (Parsons et al. 1984).

† Not significantly correlated (P>0.05).

could represent a significant, but largely unappreciated, energy resource for chemoautotrophic nitrifying bacteria in dark, oxic, receiving waters, thereby contributing to localized OC production as well as DIC and O_2 consumption within the estuary. More systematic field studies are warranted to establish the importance of this process in carbon and nitrogen cycling within urbanized estuaries.

Influence of river discharge—Significant differences in DOC and bacterial biomass pools and in some fluxes were apparent between 1997 and 1998. River discharge (q) appears to be a key difference between these years, being lower in the 1997 field season (1 Mar and 31 Oct) than in 1998 (Fig. 3A). As reported by Alpine and Cloern (1992) for the San Francisco Bay estuary, freshwater discharge appears to be very important in controlling the balance between autotrophic and heterotrophic processes because it can govern the light environment and affect the proportions of autochthonous to allochthonous input to the estuary. In our study, a significant positive correlation was found between q and light attenuation, and negative correlations were found between q and phytoplankton biomass and NPP (Table 1). Furthermore, concentrations of PO_4^{3-} and NO_2^- (nutrients putatively related to urban/suburban point sources) correlated negatively with q, illustrating the dilution effect of q on point sources. Planktonic respiration and DCA were both negatively correlated with q (Table 1), perhaps because these processes are stimulated by point source contributions. Freshwater discharge in concert with tidal variations alter residence times of water in the estuary and thereby govern the amounts of material processed internally or exported from the estuary. However, regression analysis revealed that variances of only a few variables (respiration, NPP, DCA, NH_4^+, NO_2^-) were predictably related to q and only marginally so (r^2 = 0.20–0.47).

Similar to Howarth et al.'s (2000) observations on primary production in the HRE, our data suggest that low and high flow regimes represent two distinct states for carbon dynam-
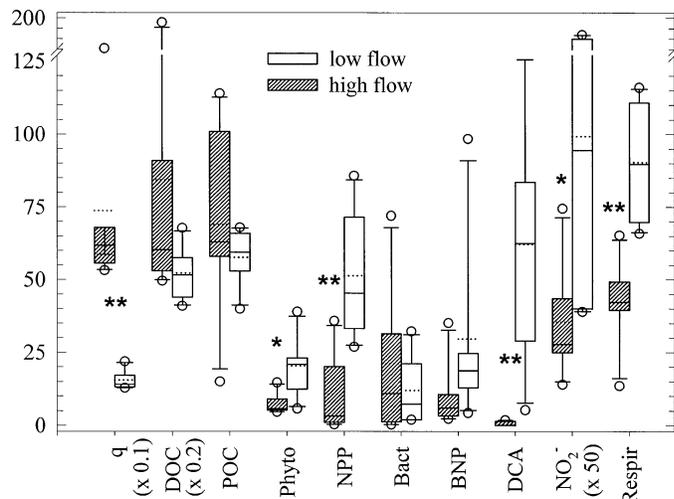
Fig. 11. Effects of river discharge on organic carbon pools (DOC, POC, phytoplankton, and bacteria, μmol C L^{-1}) and biological processes (NPP, BNP, DCA, and respiration, mmol C m^{-2} d^{-1}; NO_2^-, μmol L^{-1}) in the surface mixed layer of station HB only. Observations for high (>250 m^3 s^{-1}) and low (<250 m^3 s^{-1}) flow presented in hatched and open boxes, respectively. Boxes enclose 75% of all observations; solid and dotted lines within boxes denote medians and means, respectively; whiskers represent the 90th percentiles; and open circles denote outliers. Significant differences were determined by t-test or Mann–Whitney rank sum test, depending on normality of data: * $p < 0.05$, ** $p < 0.005$.

ics in the HRE. To illustrate, results from HB were sorted into low- and high-flow observations using $q = 250$ m^3 s^{-1} as the transition point ($n = 6$ for both) (Fig. 11). Doing so explained variance in the data to a greater degree than did either regression analysis or interannual comparisons. Under high flow conditions, means for DOC, POC, and bacterioplankton concentrations were 1.6-, 1.2-, and 1.8-fold higher than under low flow, and their ranges were wider. In contrast, high-flow means for phytoplankton biomass, NPP, DCA, NO_2^- concentrations, and respiration were significantly (0.001 < p < 0.05) less than means during the low flow regime by factors of 2.7, 4.8, 113, 2.8, and 2.1, respectively (Fig. 11). These trends suggest that low flow conditions (1) promote primary production, probably by partial relief from light limitation; (2) decrease dilution of point source materials, (3) stimulate BNP and respiration by providing higher concentrations of labile OC, and (4) favor DCA, presumably through nitrification, because NH_4^+ and NO_2^- concentrations are elevated. Trends further suggest that, even though more plentiful, bacteria encountered under high flow conditions are less active (i.e., lower production and respiration). Freshwater discharge, like temperature, appears to be a master variable, exerting significant influence over carbon dynamics and trophic status of the HRE.

Carbon budget—To assess internal carbon processing and export from the lower HRE, we estimated OC inflow, outflow, and turnover using surface water discharge, DOC and POC pools, and biological carbon fluxes. Under low flow conditions, DOC loadings in surface waters increased from 17 to 30 × 10^6 mol C d^{-1} between HB and VN (Table 2).

Table 2. Median loadings* of organic carbon pools in the surface mixed layer of the Hudson River estuary under low and high flow conditions ($\times 10^6$ mol C d^{-1}). Low flow conditions defined as freshwater discharge, $q<250$ m^3 d^{-1} at Troy Dam ($n=6$ for both conditions and medians = 140 and 619 m^3 s^{-1}). Annual totals ($\times 10^6$ mol C yr^{-1}) estimated by applying low and high flow scalars to daily freshwater discharges.

Site	Flow	DOC	ΔDOC	POC	ΔPOC	Phy + Bac	Δ(P + B)
HB (65 rkm)	Low	17		4.1		1.6	
	High	56		9.6		2.9	
	Annual	16,300		3,000		970	
GT (15 rkm)	Low	9	−8	3.8	−0.3	1.3	−0.3
	High	38	−18	8.5	−1.1	2.0	−0.9
	Annual	10,600	−5,700	2,700	−300	700	−270
VN (−13 rkm)	Low	30	+21	6.3	+2.5	3.9	+2.6
	High	83	+45	16.0	+7.5	7.4	+5.4
	Annual	24,900	+14,300	4,900	+2,200	2,400	+1,700

* Loadings estimates based on (1) freshwater discharge, q, at Troy Dam; (2) q representing 65% of freshwater input at HB and GT and 57% at VN ($q_{corr} = q/0.65$ or $q/0.57$) (Howarth et al. 1991; Brosnan and O'Shea 1996); (3) basin equation approach for total surface water discharge, Q, assuming water and salt conservation, $Q = q_{corr}(S_{bot}/[S_{bot} - S_{surf}])$, where S_{bot} and S_{surf} equal salinities in bottom and surface waters; and (4) medians of OC pool sizes. Medians used to avoid undue influence of outliers among heteroscedastic data.

This trend suggests that DOC is introduced into the estuary by several possible sources, including autochthonous production, benthic fluxes, small tributaries, surface runoff, and point sources. Between low and high flow, DOC loadings increased ~3.4-fold, while median freshwater discharge increased 4.4-fold. Under high flow conditions, DOC loadings decreased by 18×10^6 mol C d^{-1} between HB and GT and then increased by 45×10^6 mol C d^{-1} between GT and VN. This might reflect net consumption of DOC by biological uptake or partial removal by chemical flocculation in the upper segment, accompanied by significant allochthonous input in the lower segment.

Like DOC, POC loadings decreased in the upper segment (HB–GT), increased in the lower segment (GT–VN), and increased with q (Table 2). POC represented 4 to 52% (mean = 19%) of the TOC discharged, not the 50% often assumed for many other estuaries (Smith and Hollibaugh 1993). Ignoring higher trophic levels, inventories of phytoplankton and bacterial biomass alone accounted for significant fractions of the total POC pool, with estimates varying from 7 to >100%. The mean proportions of POC represented by the sum of phytoplankton and bacterioplankton in surface waters were similar at HB and VN (57 and 59%, respectively) and markedly lower at GT (33%), suggesting different sources of particulate carbon in this part of the estuary. However, particulate C:N ratios were not significantly different ($p \gg 0.05$) between stations, averaging 14.2 (atomic) (not presented). Although the relationships between cellular carbon and Chl a or bacterial volumes can vary within the system, these comparisons illustrate that a nontrivial portion of the POC is comprised of algal and bacterial biomass and that qualitative differences in POC between stations might not be evident from bulk elemental analyses. Under both flow conditions, loadings of planktonic biomass were nearly equivalent at HB and GT but increased more than 3-fold as surface waters reached VN, presumably because of enhanced biological production in the lower segment.

Areal planktonic production (NPP + DCA + BNP) increased from HB to VN under both flow regimes (Table 3). Estimates of community respiration were high at HB, decreased at GT, and then increased at VN under both flow conditions (Table 3). The ratio of autotrophic production to respiration (P:R) varied from 0.01 to 0.63, was highest at GT during low flow, and increased seaward during high flow. Total production and respiration during low flow conditions were consistently higher than during high flow by factors of 6.1–21.2 and 1.3–2.1, respectively. Apparently much more carbon was processed within the estuary when hydrologic residence times were longer.

Net production of DIC reflects the balance between two processes: CO_2 production by community respiration and CO_2 consumption by autotrophs (light and dark DIC assimilation). This net flux varied less predictably with location and river discharge than other variables. For example, even though respiration at GT under low flow conditions was higher than during high flow, net DIC production was diminished as a consequence of elevated autotrophic consumption (Table 3). In contrast, net DIC production at VN was virtually indistinguishable between flow conditions (372–377 mmol C m^{-2} d^{-1}). Respiration, photoautotrophy, and chemoautotrophy are differentially controlled by several environmental factors that can vary independently, including temperature, labile C, nutrient speciation, and light exposure. Consequently, net DIC production is difficult to predict by indirect means in complex estuarine systems, such as the Hudson.

As a first approximation of internal processing of carbon for the Hudson mainstem, the estuary was divided into two segments (HB–GT and GT–VN). Median planktonic production and respiration values for the surface mixed layer were multiplied by estimates of that segment's surface area (Table 4), acknowledging that our data does not adequately address spatial variability. Under median low flow conditions, these estimates suggest that the entire estuary (174 km^2) produced 35×10^6 mol C d^{-1} of biomass and respired 96×10^6 mol C d^{-1}. In contrast, under high flow conditions mean production and respiration were 3×10^6 and 52×10^6 mol C d^{-1}, respectively. Thus, under low flow conditions, the estuary processes ~2.4 times more carbon (biological production and respiration) than under high flow (Table 4).

Table 3. Median* planktonic carbon fluxes in surface waters of the Hudson River estuary under low and high flow conditions.

Site	Flow	Auto- + heterotrophic production† (mmol C m^{-2} d^{-1})	BNP:NPP	Community respiration‡ (mmol C m^{-2} d^{-1})	P:R§	Net DIC flux‖ (mmol C m^{-2} d^{-1})
HB (65 rkm)	Low	132	0.33	818	0.14	735
	High	8	1.08	390	0.01	385
GT (15 rkm)	Low	212	0.19	360	0.63	61
	High	10	0.40	204	0.04	205
VN (−13 rkm)	Low	336	0.23	553	0.37	377
	High	55	0.37	418	0.11	372

* Estimates of planktonic carbon fluxes derived from medians of six low- and six high-flow samples.

† Includes photoautotrophic (diurnal NPP), chemoautotrophic (dark DIC assimilation), and heterotrophic (BNP) production of organic matter for surface mixed layer only (BNP is mean of ^{3}H-leucine and ^{3}H-thymidine methods.).

‡ Includes data for surface mixed layer and approximately the <5.0-μm size fraction only. Oxygen consumption data converted to CO_2 production using an RQ of 0.70 (see text).

§ P:R ratio of autotrophic production (diurnal NPP + dark DIC assimilation) to respiration, indicative of net DIC balance (i.e., values <1.00 denote net biological production of DIC).

‖ Difference between respiration (measured respiration + estimated phytoplankton R) and autotrophic DIC assimilation (light + dark). Estimated phytoplankton R on average contributed <3% to total respiration (range = 0.1–11%).

This is nearly balanced by the export of 2.7 times less OC from the estuary on the basis of independent estimates of TOC loadings at VN (Table 2).

Annual carbon budgets were estimated by scaling median OC pools and biological fluxes with daily observed river discharge for the periods of 17 Oct 96 to 16 Oct 97 and 17 Oct 97 to 16 Oct 98. Because this segment of the estuary remained ice free throughout our study, we assume that metabolism continued through the winter. This assumption is supported by the significant bacterial production evident in our earliest spring observations and in a previous study (Sañudo-Wilhelmy and Taylor 1999) when water temperatures were 4.5 to 5.2°C, suggesting that active psychrotolerant communities inhabit the HRE. Low flow scalars from Tables 2 and 3 were applied for all days when freshwater discharge, q, was below 250 m^3 s^{-1} at Troy Dam and high flow scalars to those days with higher discharges. No significant differences were observed between the two annual budgets, suggesting that interannual differences reported above did, in fact, arise from timing of sampling. Thus, only the average annual budget results are presented.

According to this conservative analysis, 19,300 × 10^6 mol C of TOC (DOC + POC) enters the saline portion of the estuary at HB annually (Table 2). Over the same time interval, 29,800 × 10^6 mol C of TOC passes through the Verrazano Narrows into lower New York Bay and Mid-Atlantic Bight. Thus, TOC loadings actually increase by 10,500 × 10^6 mol C as surface waters pass through the study area. Our estimate of total planktonic production within the system was ~5,600 × 10^6 mol C yr^{-1} during both years (Table 4). On an annual basis, autotrophic C fixation (photo- and chemoautotrophic) accounted for 55, 77, and 82% of total microplanktonic production at HB, GT, and VN, respectively, or ~72% systemwide. Consequently, autotrophic processes can potentially account for 37% of the estimated TOC gain. The remaining 63% of the TOC accumulation must be attributed to allochthonous input of OC because heterotrophic bacterial production merely transforms preformed OC pools. Entrainment of bottom waters during tidal mixing could el-

evate surface OC loadings as well. However, TOC pools in bottom waters and the halocline were systematically lower than in surface waters and would therefore dilute surface TOC loadings in most cases.

Our estimates of TOC inflow to the saline HRE exceed previous estimates of 4,100–7,400 × 10^6 mol C yr^{-1} (49,600–89,900 MT C yr^{-1}) exported from the tidal freshwater Hudson (Howarth et al. 1996). Those estimates were based on freshwater discharge rates (q) through rkm 100, which varied from 14 to 19 × 10^9 m^3 yr^{-1}, and match our estimates of 14–16 × 10^9 m^3 yr^{-1}. However, our import es-

Table 4. Model results for biological fluxes of carbon in two segments of the Hudson River estuary.

	Flow	HB–GT segment	GT–VN segment	HB–VN
Area (km^2)*		118	56	174
Production†	Low	20	15	35
(×10^6 mol C d^{-1})	High	1	2	3
(×10^6 mol C yr^{-1})	Annual‡	3,000	2,600	5,600
Respiration†	Low	70	26	96
(×10^6 mol C d^{-1})	High	35	17	52
(×10^6 mol C yr^{-1})	Annual	18,600	7,900	26,500
Mean P:R§		0.20	0.29	0.22
Net DIC flux‖	Low	47	12	59
(×10^6 mol C d^{-1})	High	35	16	51
(×10^6 mol C yr^{-1})	Annual	15,400	5,800	21,200

* Estimates of river segment surface areas derived from deAngelis and Scranton (1993).

† Measured microplanktonic production and respiration within segments are estimated from products of averages between stations (HB and GT or GT and VN from Table 3) and segment surface areas. Rates for the entire study area (HB–VN) are sums of the segments.

‡ Annual fluxes estimated by applying low and high flow scalars to daily river freshwater discharges, q.

§ Median of daily P:R estimates scaled to river discharge as discussed above and as defined in Table 3.

‖ Net production of dissolved inorganic carbon within segments calculated from balance between respiration (measured + phytoplankton estimate) and autotrophic DIC assimilation (light and dark).

timate is based on total surface layer flows (Q) at rkm 65, which were $45–47 \times 10^9$ m^3 yr^{-1} and included entrained seawater. Normalizing our TOC loadings data to q produces an import loading of $\sim$6,000 $\times 10^6$ mol C yr^{-1}, midrange of export loadings reported by Howarth et al. (1996). It is interesting to note that zebra mussels (*Dreissena polymorpha*) invaded the tidal freshwater Hudson above 100 rkm in 1991, after Howarth et al.'s (1996) field study in 1988 and before the present study. Major ecological alterations have been documented in the affected area since the invasion (Caraco et al. 2000), but effects on the transport and quality of OC entering the estuary are unknown.

Within surface waters, total biological processing of carbon in our study area amounted to $\sim$32,100 $\times 10^6$ mol C annually, of which 26,500 $\times 10^6$ mol C was respired to CO$_2$ (Table 4). Because autotrophic DIC assimilation was $\sim$4,000 $\times 10^6$ mol C, a minimum of 38,600 $\times 10^6$ mol of OC (32,100 [biological fluxes] + 10,500 [TOC gain] − 4,000 [autotrophic C fixation]) must enter the system annually from the shoreline. Clearly urban runoff and point sources cannot be ignored. Under low flow conditions, discharge from municipal point sources alone can account for up to 40% of the estuary's total freshwater budget (Clark et al. 1995). Of the average freshwater discharge through Verrazano Narrows, $\sim$81% originates from the Hudson mainstem and from tributaries in New York and New Jersey. The remaining 19% is derived from 49 municipal point sources (13.8%), 1,000 storm water outfalls (3.6%), $\sim$650 combined sewer overflow outfalls (1.3%), and $\sim$400 direct industrial discharges (0.3%) (HydroQual 1991). Therefore, a multitude of highly variable and poorly characterized sources of OC from the urban watershed can contribute significantly to this estuary's carbon and freshwater budgets. Our rudimentary budget includes OC derived from point sources and processed in surface waters, but insufficient information is available to accurately quantify freshwater discharges from these sources. We believe our estimates of OC export from the saline HRE to the coastal ocean are the first to be reported and are somewhat conservative because of the uncertainty associated with Q at station VN.

DIC export to the coastal ocean and atmosphere also must be significant because combined photo- and chemoautotrophic production can consume only $\sim$22% of respiratory CO$_2$ produced biologically within the system (Table 4). In fact, our estimated annual budget suggests that the HRE produces DIC excesses of at least 21,200 $\times 10^6$ mol C yr^{-1}. This production rate equates to median turnover times of 15–21 d for DIC pools among the stations. However, the amounts of this DIC that will evade to the atmosphere or advect seaward are uncertain. CO$_2$ evasion from surface waters of other estuaries appears to be a dominant pathway for respiratory carbon (Kempe 1982; Frankignoulle et al. 1998; Raymond et al. 2000). In the York River estuary, for example, estimates of CO$_2$ evasion varied from 5 to 45 mmol CO$_2$ m^{-2} d^{-1} and usually surpassed DIC advection from the study site (Raymond et al. 2000). In the tidal freshwater Hudson itself, pCO$_2$ values were always supersaturated, sometimes by a factor of four, and estimates of CO$_2$ evasion varied from 0 to $\sim$70 mmol CO$_2$ m^{-2} d^{-1} over an annual cycle, averaging 5.8–13.5 mol CO$_2$ m^{-2} yr^{-1} (Raymond et al. 1997). Even

higher CO$_2$ evasion rates were reported for nine urbanized European estuaries, which averaged 170 mmol CO$_2$ m^{-2} d^{-1} (Frankignoulle et al. 1998). However, our average DIC production rates (330 mmol C m^{-2} d^{-1} or 120 mol C m^{-2} yr^{-1}) are as much as 66-fold higher than reported CO$_2$ evasion rates.

We have no direct measurements of pH, pCO$_2$, alkalinity, or wind mixing, so CO$_2$ evasion rates can not be accurately estimated. Given the complex nature of inputs to this estuary, the carbonate chemistry could vary spatially and temporally, favoring or inhibiting CO$_2$ evasion from place to place. Even with high, constant total DIC concentrations, small variations in pH can shift the system from undersaturated to supersaturated with CO$_2$, because pCO$_2$ decreases exponentially with rising pH. Although the fate of CO$_2$ produced in the HRE cannot be determined directly, the observed DIC production rates appear sufficient to support CO$_2$ evasion rates similar to those reported elsewhere, as well as export of large amounts of DIC out of the estuary. Resolution of the fate of DIC produced in this estuary awaits further research.

Summary—We have demonstrated that, like a growing number of reports for aquatic systems, the HRE usually has a net heterotrophic balance, in which carbon oxidative processes outpace carbon reductive processes. Instances of net autotrophy in the plankton appear to be strongly influenced by dark DIC assimilation, putatively driven by nitrification. Our data suggest that planktonic carbon processing and trophic status within the estuary are largely controlled by river discharge. The low flow regime provides better light and inorganic nutrient conditions for autotrophs than high flows, thereby promoting relatively high biological production (auto- and heterotrophic) and respiration, resulting in modest TOC export to the ocean. In contrast, environmental conditions during high flow regimes diminish internal biological production and metabolism and promote higher TOC export to the ocean. Carbon budgets suggest that $\sim$19 $\times 10^9$ mol TOC enters the estuary from the Hudson River, 39 $\times 10^9$ mol TOC enters between HB and VN, and 30 $\times 10^9$ mol TOC is exported to the ocean annually. This estuary also has a net production of $\sim$21 $\times 10^9$ mol DIC yr^{-1}, of which undetermined portions advect seaward and evade to the atmosphere as CO$_2$.

References

ALPINE, A. E., AND J. E. CLOERN. 1992. Trophic interactions and direct physical effects control phytoplankton biomass and production in an estuary. Limnol. Oceanogr. **37:** 946–955.

ANDERSON, L. A. 1995. On the hydrogen and oxygen content of marine phytoplankton. Deep-Sea Res. **42:** 1675–1680.

ARNOLD, C. L. 1982. Modes of fine-grained suspended sediment transport in the Hudson River estuary. M.S. thesis, State University of New York, Stony Brook.

BELL, R. T. 1993. Estimating production of heterotrophic bacterioplankton via incorporation of tritiated thymidine, p. 495–504. *In* P. F. Kemp, B. F. Sherr, E. B. Sherr, and J. J. Cole [eds.], Handbook of methods in aquatic microbial ecology. Lewis.

BILLEN, G. 1975. Nitrification in the Scheldt estuary (Belgium and the Netherlands). Estuar. Coast. Mar. Sci. **3:** 79–89.

BROSNAN, T. M., AND M. L. O'SHEA. 1996. Long-term improvements in water quality due to sewage abatement in the lower Hudson River. Estuaries **19:** 890–900.

CARACO, N. F., J. J. COLE, S. E. G. FINDLAY, D. T. FISCHER, G. G. LAMPMAN, M. L. PACE, AND D. L. STRAYER. 2000. Dissolved oxygen declines in the Hudson River associated with the invasion of the Zebra Mussel (*Dreissena polymorpha*). Environ. Sci. Technol. **34:** 1204–1210.

CLARK, J. F., H. J. SIMPSON, R. F. BOPP, AND B. DECK. 1992. Geochemistry and loading history of phosphate and silicate in the Hudson estuary. Estuar. Coast. Shelf Sci. **34:** 213–233.

———, W. M. SMETHIE, AND H. J. SIMPSON. 1995. Chlorofluorocarbons in the Hudson estuary during summer months. Water Res. **31:** 2553–2560.

COFFIN, R. B., J. P. CONNOLLY, AND P. S. HARRIS. 1993. Availability of dissolved organic carbon to bacterioplankton examined by oxygen utilization. Mar. Ecol. Prog. Ser. **101:** 9–22.

COLE, J. J., N. F. CARACO, AND B. PEIERLS. 1991. Phytoplankton primary production in the tidal, freshwater Hudson River, New York (USA). Verh. Int. Ver. Limnol. **24:** 1715–1719.

———, ———, AND ———. 1992. Can phytoplankton maintain a positive carbon balance in a turbid, freshwater tidal estuary? Limnol. Oceanogr. **37:** 1608–1617.

DEANGELIS, M. A., AND M. I. SCRANTON. 1993. Fate of methane in the Hudson River and estuary. Glob. Biogeochem. Cycles **7:** 509–523.

DEL GIORGIO, P. A., J. J. COLE, N. F. CARACO, AND R. H. PETERS. 1999. Linking planktonic biomass and metabolism to net gas fluxes in northern temperate lakes. Ecology **80:** 1422–1431.

FINDLAY, S., M. L. PACE, D. LINTS, J. J. COLE, N. F. CARACO, AND B. PEIERLS. 1991. Weak coupling of bacterial and algal production in a heterotrophic ecosystem: The Hudson River estuary. Limnol. Oceanogr. **36:** 268–278.

FRANKIGNOULLE, M., I. BOURGE, AND R. WOLLAST. 1996. Atmospheric CO_2 fluxes in a highly polluted estuary (the Scheldt). Limnol. Oceanogr. **41:** 365–369.

———, AND OTHERS. 1998. Carbon dioxide emission from European estuaries. Science **282:** 434–436.

FUKUDA, R., H. OGAWA, T. NAGATA, AND I. KOIKE. 1998. Direct determination of carbon and nitrogen contents of natural bacterial assemblages in marine environments. Appl. Environ. Microbiol. **64:** 3352–3358.

HOPKINSON, C. S., A. E. GIBLIN, R. H. GARRITT, J. TUCKER, AND M. A. J. HULLAR. 1998. Influence of the benthos on growth of planktonic estuarine bacteria. Aquat. Microb. Ecol. **16:** 109–118.

HOWARTH, R. W., J. R. FRUCI, AND D. SHERMAN. 1991. Inputs of sediment and carbon to an estuarine ecosystem: Influence of land use. Ecol. Appl. **1:** 27–39.

———, R. MARINO, R. GARRITT, AND D. SHERMAN. 1992. Ecosystem respiration and organic carbon processing in a large, tidally influenced river: The Hudson River. Biogeochemistry **16:** 83–102.

———, R. SCHNEIDER, AND D. SWANEY. 1996. Metabolism and organic carbon fluxes in the tidal freshwater Hudson River. Estuaries **19:** 848–865.

———, D. P. SWANEY, T. J. BUTLER, AND R. MARINO. 2000. Climatic control on eutrophication of the Hudson River estuary. Ecosystems **3:** 210–215.

HYDROQUAL, INC. 1991. Assessment of pollutant loadings to NY/NJ Harbor. Submitted to EPA Region II, for Task 7.1, NY/NJ Harbor estuary Program, New York, N.Y.

ITTEKKOT, V. 1988. Global trends in the nature of organic matter in river suspensions. Nature **332:** 436–438.

JENSEN, L. M., K. SAND-JENSEN, S. MARCHER, AND M. HANSEN.

1990. Plankton community respiration along a nutrient gradient in a shallow Danish estuary. Mar. Ecol. Prog. Ser. **61:** 75–85.

KEMPE, S. 1982. Long-term records of CO_2 pressure fluctuations in fresh water. Mitt. Geol-Paleontol Instit. Univ. Hambg. **52:** 91–332.

———. 1984. Sinks of the anthropogenically enhanced carbon cycle in surface fresh waters. J. Geophys. Res. **89:** 4657–4676.

KIRCHMAN, D. L. 1993. Leucine incorporation as a measure of biomass production by heterotrophic bacteria, p. 509–512. *In* P. F. Kemp, B. F. Sherr, E. B. Sherr, and J. J. Cole [eds.], Handbook of methods in aquatic microbial ecology. Lewis.

KOSEFF, J. R., J. K. HOLEN, S. G. MONISMITH, AND J. E. CLOERN. 1993. Coupled effects of vertical mixing and benthic grazing on phytoplankton populations in shallow, turbid estuaries. J. Mar. Res. **51:** 843–868.

LI, W. K. W. 1982. Estimating heterotrophic bacterial productivity by inorganic radiocarbon uptake: Importance of establishing time courses of uptake. Mar. Ecol. Prog. Ser. **8:** 167–172.

LUCAS, L. V., J. E. CLOERN, J. R. KOSEFF, S. G. MONISMITH, AND J. K. THOMPSON. 1998. Does the Sverdrup critical depth model explain bloom dynamics in estuaries? J. Mar. Res. **56:** 375–415.

MALONE, T. C. 1977. Environmental regulation of phytoplankton productivity in the lower Hudson estuary. Estuar. Coast. Mar. Sci. **5:** 157–171.

MARTIN, J. H. 1993. Determination of particulate organic carbon (POC) and nitrogen (PON) in seawater, p. 37–40. *In* S. Kadar, M. Leinen and J. W. Murray [eds.], United States Joint Global Ocean Flux Study: Equatorial Pacific Study—sampling and analytical protocols. U. S. JGOFS, Woods Hole.

———, G. A. KNAUER, D. M. KARL, AND W. W. BROENKOW. 1987. VERTEX: Carbon cycling in the northeast Pacific. Deep-Sea Res. **34:** 267–285.

MCELROY, M. B., J. W. ELKINS, S. C. WOLFSY, C. E. KOLB, A. P. DURAIN, AND W. A. KAPLAN. 1978. Production and release of N_2O from the Potomac estuary. Limnol. Oceanogr. **23:** 1168–1182.

NORLAND, S. 1993. The relationship between biomass and volume of bacteria, p. 303–308. *In* P. F. Kemp, B. F. Sherr, E. B. Sherr, and J. J. Cole [eds.], Handbook of methods in aquatic microbial ecology. Lewis.

PARSONS, T. R., Y. MAITA, AND C. M. LALLI. 1984. A manual of chemical and biological methods for seawater analysis. Pergamon.

PILGRIM, D. A. 1987. Measurement and estimation of the extinction coefficient in turbid estuarine waters. Cont. Shelf Res. **7:** 1425–1428.

PORTER, K. G., AND Y. S. FEIG. 1980. The use of DAPI for identifying and counting microflora. Limnol. Oceanogr. **25:** 943–948.

RAYMOND, P. A., AND J. E. BAUER. 2000. Bacterial consumption of DOC during transport through a temperate estuary. Aquat. Microb. Ecol. **22:** 1–12.

———, N. F. CARACO, AND J. J. COLE. 1997. Carbon dioxide concentration and atmospheric flux in the Hudson River. Estuaries **20:** 381–390.

———, J. E. BAUER, AND J. J. COLE. 2000. Atmospheric CO_2 evasion, dissolved inorganic carbon production and net heterotrophy in the York River estuary. Limnol. Oceanogr. **45:** 1707–1717.

REDFIELD, A. C., B. H. KETCHUM, AND F. A. RICHARDS. 1963. The influence of organisms on the composition of seawater, p. 26–77. *In* M. N. Hill [ed.], The sea. V. 2. Interscience.

RICE, W. R. 1989. Analyzing tables of statistical tests. Evolution **43:** 223–225.

ROBINSON, C., AND P. J. LEB. WILLIAMS. 1999. Plankton net com-

munity production and dark respiration in the Arabian Sea during September 1994. Deep-Sea Res. **46:** 745–765.

———, S. D. ARCHER, AND P. J. LEB. WILLIAMS. 1999. Microbial dynamics in coastal waters of East Antarctica: Plankton production and respiration. Mar. Ecol. Prog. Ser. **180:** 23–36.

SAÑUDO-WILHELMY, S., AND G. T. TAYLOR. 1999. Bacterioplankton dynamics and organic carbon partitioning in the lower Hudson River estuary. Mar. Ecol. Prog. Ser. **182:** 17–27.

SHARP, J. H., R. BENNER, L. BENNETT, C. A. CARLSON, S. E. FITZWATER, E. T. PELTZER, AND L. M. TUPAS. 1995. Analyses of dissolved organic carbon in seawater—the JGOFS EQPAC methods comparison. Marine Chem. **48:** 91–108.

SIMON, M., AND F. AZAM. 1989. Protein content and protein synthesis rates of planktonic marine bacteria. Mar. Ecol. Prog. Ser. **51:** 201–213.

SMITH, S. V., AND J. T. HOLLIBAUGH. 1993. Coastal metabolism and the oceanic organic carbon balance. Rev. Geophys. **31:** 75–89.

———, AND F. T. MACKENZIE. 1987. The ocean as a net heterotrophic system: Implications from the carbon biogeochemical cycle. Glob. Biogeochem. Cycles **1:** 187–198.

SØNDERGAARD, M., AND M. MIDDELBOE. 1995. A cross-system analysis of labile dissolved organic carbon. Mar. Ecol. Prog. Ser. **118:** 283–294.

———, AND OTHERS. 2000. Net accumulation and flux of dissolved organic carbon and dissolved organic nitrogen in marine planktonic communities. Limnol. Oceanogr. **45:** 1097–1111.

SPITZY, A., AND J. LEENHEER. 1991. Dissolved organic carbon in rivers, p. 213–232. *In* E. T. Degens, S. Kempe, and J. E. Richey [eds.], Biogeochemistry of major world rivers. Wiley.

STRATHMANN, R. R. 1967. Estimating the organic carbon content of phytoplankton from cell volume or plasma volume. Limnol. Oceanogr. **12:** 411–418.

SUSZKOWSKI, D. J. 1990. Conditions in the NY/NJ Harbor estuary. *In* Proceedings of Cleaning Up Our Coastal Waters: An Unfinished Agenda. Manhattan College, Riverdale, New York, 12–14 Mar 90.

SWANEY, D. P., R. W. HOWARTH, AND T. J. BUTLER. 1999. A novel approach for estimating ecosystem production and respiration in estuaries: Application to the oligohaline and mesohaline Hudson River. Limnol. Oceanogr. **44:** 1509–1521.

TAKAHASHI, T., W. S. BROECKER, AND S. LANGER. 1985. Redfield ratio estimates based on chemical data from isopycnal surfaces. J. Geophys. Res. **90:** 6907–6924.

TANTICHODOK, P. 1990. Relative importance of phytoplankton and organic detritus for the suspension feeding bivalve, *Mytilus edulis* L. in Long Island Sound. Ph.D. dissertation, State Univ. of New York, Stony Brook.